Backward production of light ions in the interaction of 400 GeV protons with nuclei

S. Frankel, W. Frati, and M. Gazzaly
University of Pennsylvania, Philadelphia, Pennsylvania

Y. D. Bayukov, V. I. Efremenko, G. A. Leksin, N. A. Nikiforov, V. I. Tchistilin, and Y. M. Zaitsev
Institute of Theoretical and Experimental Physics, Moscow, U.S.S.R.

C. F. Perdrisat
College of William and Mary, Williamsburg, Virginia
(Received 2 August 1979)

Measurements of the invariant cross sections for the reaction $p(400\ \text{GeV}) + (^6\text{Li}, \text{Be}, \text{C}, \text{Al}, \text{Cu}, \text{Ta}) \rightarrow (d, t, ^3\text{He}, ^4\text{He}) + X$ at laboratory angles of 70, 90, 118, 137, and 160° are reported. Comparisons are made using several scaling variables.

[NUCLEAR REACTIONS Inclusive cross section; 400 GeV incident protons; ^{6}Li, Be, C, Al, Cu, Ta targets; production of d, t, ^{3}He, ^{4}He; Lab angles 70°, 90°, 118°, 137°, and 160°.]

INTRODUCTION

Inclusive cross sections for the production of protons at backward angles, which are forbidden in the interaction of protons with free stationary nucleons, are believed to contain the basic information needed for the study of the high momentum components of nuclear wave functions or of collective phenomena in nuclei. Such data have been treated in the framework of single particle interactions with nucleons of high momentum[1-4] within the nucleus, and from the interaction of the incident projectile with "clusters" of nuclear matter.[5-9]

The production of *outgoing* clusters of nucleons, whether they are unbound or bound, as in (p, d) reactions, ought to be intimately related to mechanisms of the basic (p, p) reaction itself. In a single scattering model, with the scattered proton picking up a nucleon to form a deuteron, the mechanism is in fact a "final state interaction" so one would eventually require that both proton and composite particle production emerge from a model of hard scattering dressed with final state interactions. In cluster models the nucleon clusters are not only postulated to explain proton backscattering but may be needed to account for direct ejection of composites by the incoming probe.

The production of the simplest composite such as the deuteron, may indeed require a very complete understanding. Because of this it is desirable to have at hand data on the production of other composites (t, ^{3}He, ^{4}He, etc.) as well, as testing grounds for the various theories. Similar data on large invariant masses can also, in principal, come from reactions which scan a continuous range of invariant masses, but, at present, little data of this type is available. In this paper we report on the results of our 400 GeV studies of the reaction $p(400\ \text{GeV}) + (^6\text{Li}, \text{Be}, \text{C}, \text{Al}, \text{Cu}, \text{Ta}) \rightarrow (d, t, ^3\text{He}, ^4\text{He}) + X$. The measurements were made at 70, 90, 118, 137, and 160°, laboratory.

MEASUREMENT TECHNIQUE

The experimental apparatus has been described in detail previously[10] so only the barest outlines are presented here. A spectrometer of momentum resolution $\Delta p/p = 5.8\%$ and an integrated product of resolution times acceptance of 0.069 msr was used to detect the protons and light ions originating in our targets. Separation of these particles into the various types was made with the use of time of flight and dE/dx measurements. The main difference in the handling of the proton and the light ion data is that corrections for energy loss in the targets were generally larger for the ions. Estimates of the nuclear absorption of the ions in the thicker targets were made using the data in Millburn *et al.*[11] For the thickest target (Be) the largest correction was 8.6% for deuterons and 7.9% for alpha particles.

DATA PRESENTATION

This is the first experiment on the backward production of composite particles at a bombarding energy of 400 GeV. There are as yet no detailed predictions for this region although there are many models that could be extended to compare with these new data. Thus these data are presented

TABLE I. $d\sigma = Ed^3\sigma/dp^3$ [GeV mb/sr (GeV/c)^3 nucleon] vs p = momentum (GeV/c). Laboratory angle = 70°.

Ta		Cu		Al		C		Be		^{6}Li	
p	$d\sigma$	p	$d\sigma$	p	$d\sigma$	p	$d\sigma$	p	$d\sigma$	p	$d\sigma$
Deuterons											
0.603	6.9 ±0.5	0.604	3.15 ±0.25	0.618	2.35 ±0.21	0.648	1.06 ±0.10	0.821	0.282±0.025	0.594	0.72 ±0.07
0.691	4.1 ±0.3	0.777	1.32 ±0.09	0.789	0.78 ±0.04	0.729	0.74 ±0.07	0.990	0.119±0.009	0.767	0.242±0.023
0.782	2.53 ±0.16	0.965	0.45 ±0.03	0.979	0.257±0.017	0.805	0.42 ±0.04	1.166	(0.35 ±0.03)E-1	0.960	0.105±0.008
0.978	0.89 ±0.06	1.154	0.144±0.010	1.166	(0.87 ±0.07)E-1	0.978	0.167±0.012			1.142	(0.288±0.028)E-1
1.161	0.326±0.023					1.153	(0.52 ±0.04)E-1				
Tritons											
0.701	2.30 ±0.20	0.797	0.33 ±0.04	0.811	0.133±0.012	0.799	0.133±0.028	0.893	(0.41 ±0.09)E-1	0.786	(0.47 ±0.09)E-1
0.790	1.24 ±0.10	0.977	0.100±0.011	0.992	(0.63 ±0.08)E-1	0.861	(0.53 ±0.11)E-1	1.037	(0.16 ±0.03)E-1	0.970	(0.144±0.026)E-1
0.983	0.33 ±0.03	1.161	(0.44 ±0.05)E-1	1.175	(0.208±0.027)E-1	1.012	(0.27 ±0.04)E-1	1.198	(0.43 ±0.08)E-2	1.149	(0.32 ±0.08)E-2
1.165	0.122±0.011					1.177	(0.71 ±0.12)E-2				

with the hope that they will stimulate detailed calculations or new approaches. Since we have accumulated a large quantity of data (Tables I–V) we have chosen to present selected graphical summaries to highlight many of the outstanding features. For convenience we have chosen the kinetic energy of the observed particles as the plotting variable and give invariant cross sections *per target nucleon*. ($Ed^3\sigma/dq^3$ is the notation used for the invariant differential cross section and is equal to $Ed^3\sigma/q^2dq\,d\cos\theta d\varphi$.) The kinetic energy variable T_q appears directly in (Ref. 12) so that the data can be directly compared with this model. There are four other scaling variables that have been used to study such data. One such scaling variable, which arises naturally in single scattering models, is the quasi two body scaling (QTBS) variable[2,13] $k_{\min}$. In an inclusive reaction, $k_{\min}$ is the lowest momentum of the recoiling A-A_q nucleus that allows production of an observed particle of kinetic energy T_q and atomic number A_q. Another is m^*, the lowest mass virtual cluster[5] that, by two body "elastic" scattering, can produce the same particle, for example by the reaction $p + m^* \to d + (m^* - 1)$. A third is the light cone variable x of Schmidt and Blankenbecler.[3] A fourth is the α variable of Frankfurt and Strikman.[4] At very high incident energies ($E_p \gtrsim 5$ GeV) the relationships between these variables become quite simple and (neglecting nuclear recoil) we have

$$k_{\min} \cong (-q\cos\theta + T_q), \tag{1}$$

$$m^* \cong (-q\cos\theta + T_q) + m_q = k_{\min} + m_q = (-q\cos\theta + E_q), \tag{2}$$

$$x = (-q\cos\theta + E_q)/M_a, \tag{3}$$

$$\alpha = -(-q\cos\theta + E_q)/m_p, \tag{4}$$

where q, T_q, and m_q are the momentum, kinetic energy, and mass of the observed particle, M_a is the nuclear mass of the target, and m_p is the mass of the projectile. Below about 5 GeV the variables differ considerably. Figure 1 shows a plot of m^*/x' and $(k_{\min} + m_q)/x'$, $(x' = xM_a)$, as a function of incident energy for laboratory angles of 90 and 180°, showing the approach to the asymptotic behavior displayed in Eqs. (1) and (2). Of course at 90° the variables are also identical with the variable of Ref. 12. Because all four scaling variables are essentially identical at 400 GeV we have chosen to make a few studies of our data using the variable $-q\cos\theta + T_q$.

RESULTS

Figure 2 shows invariant cross sections *per nucleon*, for the reaction $p + \mathrm{Ta} \to (d, t, {}^3\mathrm{He}, {}^4\mathrm{He})$

TABLE II. $d\sigma = Ed^3\sigma/dp^3$ [GeV mb/sr (GeV/c)^3 nucleon] vs p = momentum (GeV/c). Laboratory angle = 90°.

Ta		Cu		Al		C		Be		^{6}Li	
p	$d\sigma$	p	$d\sigma$	p	$d\sigma$	p	$d\sigma$	p	$d\sigma$	p	$d\sigma$
Deuterons											
0.582	6.7 ±0.4	0.602	2.40 ±0.12	0.590	1.33 ±0.08	0.625	0.70 ±0.04	0.636	0.458±0.026	0.598	0.401±0.027
0.603	5.26 ±0.21	0.648	1.72 ±0.10	0.644	0.90 ±0.06	0.664	0.52 ±0.03	0.677	0.299±0.018	0.639	0.294±0.026
0.656	3.50 ±0.19	0.680	1.55 ±0.10	0.669	1.06 ±0.06	0.692	0.46 ±0.04	0.705	0.311±0.024	0.670	0.234±0.023
0.686	3.30 ±0.16	0.705	1.29 ±0.07	0.690	0.92 ±0.06	0.726	0.335±0.020	0.740	0.196±0.012	0.706	0.192±0.015
0.715	2.63 ±0.16	0.985	0.214±0.018	0.719	0.78 ±0.04	0.791	0.246±0.016	0.954	(0.354±0.025)E-1	0.755	0.115±0.008
0.776	1.75 ±0.16			0.936	0.144±0.010	0.957	(0.66 ±0.04)E-1			0.933	(0.222±0.022)E-1
0.873	0.99 ±0.05					1.332	(0.44 ±0.04)E-2			1.120	(0.60 ±0.06)E-2
0.958	0.55 ±0.03									1.261	(0.18 ±0.05)E-2
1.240	(0.73 ±0.05)E-1										
1.355	(0.316±0.020)E-1										
1.410	(0.210±0.022)E-1										
Tritons											
0.692	1.72 ±0.07	0.693	0.54 ±0.05	0.705	0.27 ±0.03	0.738	0.104±0.015	0.753	(0.68 ±0.10)E-1	0.685	(0.79 ±0.13)E-1
0.781	0.96 ±0.09	0.990	(0.67 ±0.09)E-1	0.943	(0.39 ±0.05)E-1	0.821	(0.46 ±0.06)E-1	0.977	(0.77 ±0.09)E-2	0.766	(0.23 ±0.03)E-1
0.877	0.48 ±0.03					0.976	(0.142±0.014)E-1			0.939	(0.41 ±0.07)E-2
0.961	0.292±0.019					1.332	(0.124±0.012)E-2			1.123	(0.66 ±0.21)E-3
1.240	(0.40 ±0.03)E-1									1.261	(0.11 ±0.34)E-3
1.355	(0.190±0.013)E-1										
1.410	(0.117±0.015)E-1										
^{3}He											
1.036	(0.86 ±0.06)E-1	1.025	(0.35 ±0.04)E-1	1.181	(0.51 ±0.10)E-2	1.092	(0.39 ±0.07)E-2	1.119	(0.15 ±0.04)E-2	1.011	(0.15 ±0.08)E-2
1.206	(0.30 ±0.05)E-1	1.206	(0.104±0.011)E-1	1.289	(0.23 ±0.05)E-2	1.250	(0.114±0.025)E-2	1.273	(0.37 ±0.12)E-3		
1.312	(0.139±0.018)E-1	1.296	(0.55 ±0.13)E-2	1.339	(0.16 ±0.04)E-2	1.328	(0.46 ±0.23)E-3	1.354	(0.20 ±0.13)E-3		
1.426	(0.54 ±0.14)E-2	1.411	(0.30 ±0.07)E-2	1.439	(0.73 ±0.11)E-3						
1.747	(0.65 ±0.29)E-3										
1.901	(0.26 ±0.07)E-3										
^{4}He											
1.211	(0.30 ±0.05)E-1	1.227	(0.60 ±0.10)E-2	1.207	(0.12 ±0.06)E-2	1.312	(0.54 ±0.18)E-3				
1.316	(0.151±0.021)E-1	1.314	(0.22 ±0.10)E-2	1.310	(0.18 ±0.06)E-2						
1.430	(0.82 ±0.20)E-2	1.425	(0.15 ±0.05)E-2	1.359	(0.10 ±0.04)E-2						
1.749	(0.64 ±0.34)E-3			1.455	(0.45 ±0.11)E-3						
1.902	(0.42 ±0.13)E-3										

TABLE III. $d\sigma = Ed^3\sigma/dp^3$ [GeV mb/sr (GeV/c)^3 nucleon] vs p = momentum (GeV/c). Laboratory angle = 118°.

Ta		Cu		Al		C		Be		^{6}Li	
p	$d\sigma$	p	$d\sigma$	p	$d\sigma$	p	$d\sigma$	p	$d\sigma$	p	$d\sigma$
					Deuterons						
0.495	7.7 ±0.5	0.490	3.76 ±0.22	0.497	2.43 ±0.14	0.515	0.87 ±0.06	0.525	0.49 ±0.04	0.486	0.41 ±0.03
0.588	4.7 ±0.3	0.583	2.02 ±0.12	0.597	1.08 ±0.07	0.608	0.410±0.027	0.602	0.238±0.016	0.587	0.160±0.011
0.683	1.61 ±0.09	0.678	0.88 ±0.06	0.688	0.46 ±0.04	0.682	0.181±0.015	0.703	(0.79 ±0.07)E-1	0.686	(0.52 ±0.04)E-1
0.781	0.71 ±0.04	0.762	0.358±0.023	0.877	(0.67 ±0.05)E-1	0.859	(0.256±0.018)E-1	0.863	(0.111±0.008)E-1	0.760	(0.153±0.019)E-1
0.867	0.324±0.019	0.857	0.138±0.009	0.971	(0.301±0.019)E-1	0.960	(0.107±0.020)E-1	0.960	(0.50 ±0.04)E-2	0.843	(0.79 ±0.08)E-2
0.963	0.151±0.018	0.947	(0.62 ±0.04)E-1			1.182	(0.220±0.018)E-2	1.073	(0.180±0.015)E-2	0.951	(0.32 ±0.04)E-2
1.056	(0.58 ±0.04)E-1							1.166	(0.93 ±0.10)E-3	1.059	(0.108±0.020)E-2
1.161	(0.309±0.024)E-1									1.161	(0.76 ±0.12)E-3
1.425	(0.21 ±0.04)E-2										
					Tritons						
0.688	0.90 ±0.06	0.686	0.41 ±0.04	0.698	0.180±0.022	0.711	(0.46 ±0.08)E-1	0.735	(0.23 ±0.04)E-1	0.694	(0.115±0.020)E-1
0.785	0.53 ±0.04	0.769	0.155±0.013	0.882	(0.253±0.023)E-1	0.876	(0.69 ±0.08)E-2	0.883	(0.33 ±0.05)E-2	0.766	(0.37 ±0.10)E-2
0.869	0.212±0.014	0.862	(0.80 ±0.06)E-1	0.975	(0.99 ±0.09)E-2	0.973	(0.27 ±0.04)E-2	0.975	(0.103±0.016)E-2	0.845	(0.13 ±0.04)E-2
0.966	0.103±0.011	0.951	(0.296±0.024)E-1			1.190	(0.57 ±0.07)E-3	1.083	(0.41 ±0.06)E-3	0.955	(0.77 ±0.14)E-3
1.058	(0.45 ±0.04)E-1							1.176	(0.17 ±0.03)E-3	1.062	(0.22 ±0.09)E-3
1.163	(0.230±0.019)E-1									1.163	(0.20 ±0.08)E-3
1.425	(0.12 ±0.04)E-2										
					^{3}He						
0.992	(0.45 ±0.06)E-1	0.981	(0.16 ±0.04)E-1	0.995	(0.60 ±0.20)E-2	1.029	(0.11 ±0.08)E-2				
1.083	(0.25 ±0.04)E-1	1.167	(0.11 ±0.08)E-2								
1.179	(0.89 ±0.16)E-2										
1.286	(0.40 ±0.12)E-2										
					^{4}He						
1.092	(0.14 ±0.05)E-1										
1.187	(0.108±0.023)E-1										
1.290	(0.59 ±0.06)E-2										

TABLE IV. $d\sigma = Ed^3\sigma/dp^3$ [GeV mb/sr (GeV/c)^3 nucleon] vs p = momentum (GeV/c). Laboratory angle = 137°.

Ta		Cu		Al		C		Be		^{6}Li	
p	$d\sigma$	p	$d\sigma$	p	$d\sigma$	p	$d\sigma$	p	$d\sigma$	p	$d\sigma$
					Deuterons						
0.593	2.98 ±0.22	0.584	1.42 ±0.10	0.592	0.76 ±0.06	0.600	0.254±0.020	0.604	0.146±0.011	0.580	(0.84 ±0.08)E-1
0.769	0.50 ±0.03	0.763	0.242±0.014	0.772	0.119±0.007	0.779	(0.400±0.028)E-1	0.780	(0.167±0.011)E-1	0.756	(0.101±0.009)E-1
0.953	(0.76 ±0.05)E-1	0.943	(0.379±0.023)E-1	0.954	(0.165±0.011)E-1	0.955	(0.55 ±0.04)E-2	0.967	(0.239±0.016)E-2	0.958	(0.149±0.024)E-2
1.248	(0.359±0.023)E-2										
1.340	(0.123±0.007)E-2										
1.425	(0.69 ±0.13)E-3										
1.520	(0.26 ±0.07)E-3										
					Tritons						
0.773	0.378±0.024	0.769	0.124±0.009	0.779	(0.44 ±0.04)E-1	0.798	(0.102±0.011)E-1	0.803	(0.33 ±0.05)E-2	0.761	(0.24 ±0.04)E-2
0.955	(0.62 ±0.04)E-1	0.947	(0.189±0.014)E-1	0.958	(0.64 ±0.06)E-2	0.967	(0.117±0.012)E-2	0.980	(0.43 ±0.06)E-3	0.961	(0.23 ±0.11)E-3
1.248	(0.27 ±0.03)E-2										
1.340	(0.117±0.013)E-2										
1.425	(0.51 ±0.11)E-3										
1.520	(0.16 ±0.04)E-3										
					^{3}He						
0.983	(0.230±0.025)E-1										
1.074	(0.93 ±0.09)E-2										
1.179	(0.33 ±0.05)E-2										
1.263	(0.177±0.026)E-2										
					^{4}He						
1.186	(0.31 ±0.06)E-2										
1.270	(0.185±0.028)E-2										

TABLE V. $d\sigma = Ed^3\sigma/dp^3$ [GeV mb/sr (GeV/c)^3 nucleon] vs p = momentum (GeV/c). Laboratory angle = 160°.

Ta		Cu		Al		C		Be		^{6}Li	
p	$d\sigma$	p	$d\sigma$	p	$d\sigma$	p	$d\sigma$	p	$d\sigma$	p	$d\sigma$
					Deuterons						
0.484	6.1 ±0.4	0.490	2.78 ±0.16	0.496	1.54 ±0.09	0.516	0.57 ±0.04	0.520	0.288±0.023	0.490	0.257±0.02
0.593	2.52 ±0.15	0.595	1.15 ±0.09	0.602	0.59 ±0.04	0.606	0.238±0.016	0.610	0.114±0.008	0.585	(0.71 ±0.06)E-1
0.677	1.06 ±0.05	0.682	0.49 ±0.03	0.684	0.237±0.012	0.694	(0.82 ±0.04)E-1	0.696	(0.42 ±0.03)E-1	0.683	(0.213±0.025)E-1
0.777	0.393±0.018	0.773	0.187±0.011	0.771	0.100±0.006	0.781	(0.324±0.019)E-1	0.798	(0.129±0.010)E-1	0.785	(0.93 ±0.13)E-2
0.864	0.151±0.007	0.864	(0.72 ±0.05)E-1	0.875	(0.33 ±0.03)E-1	0.877	(0.113±0.011)E-1	0.874	(0.52 ±0.08)E-2	0.868	(0.15 ±0.08)E-2
0.942	(0.59 ±0.03)E-1	0.935	(0.277±0.020)E-1	0.943	(0.127±0.008)E-1	0.964	(0.47 ±0.05)E-2	0.953	(0.221±0.014)E-2	0.943	(0.79 ±0.19)E-3
1.046	(0.204±0.010)E-1					1.080	(0.136±0.021)E-2	1.146	(0.31 ±0.03)E-3	1.041	(0.51 ±0.12)E-3
1.145	(0.74 ±0.06)E-2					1.145	(0.58 ±0.05)E-3			1.142	(0.25 ±0.11)E-3
1.260	(0.223±0.015)E-2										
1.420	(0.22 ±0.06)E-3										
					Tritons						
0.682	0.78 ±0.05	0.690	0.241±0.018	0.694	(0.83 ±0.05)E-1	0.721	(0.220±0.016)E-1	0.726	(0.100±0.011)E-1	0.693	(0.65 ±0.10)E-2
0.781	0.291±0.015	0.779	(0.89 ±0.06)E-1	0.778	(0.37 ±0.03)E-1	0.801	(0.81 ±0.08)E-2	0.820	(0.31 ±0.04)E-2	0.791	(0.17 ±0.09)E-2
0.867	0.117±0.006	0.869	(0.35 ±0.03)E-1	0.880	(0.116±0.012)E-1	0.892	(0.35 ±0.04)E-2	0.892	(0.117±0.022)E-2	0.873	(0.25 ±0.25)E-3
0.944	0.50 ±0.04	0.940	(0.138±0.011)E-1	0.948	(0.43 ±0.04)E-2	0.976	(0.110±0.011)E-2	0.967	(0.35 ±0.07)E-3	0.947	(0.9 ±1.7)E-4
1.048	(0.170±0.008)E-1					1.090	(0.67 ±0.16)E-3	1.152	(0.70 ±0.22)E-4		
1.147	(0.59 ±0.04)E-2					1.153	(0.11 ±0.03)E-3				
1.260	(0.203±0.016)E-2										
1.420	(0.28 ±0.09)E-3										
					^{3}He						
0.978	(0.179±0.018)E-1										
1.148	(0.22 ±0.03)E-2										
1.365	(0.21 ±0.11)E-3										
					^{4}He						
1.157	(0.39 ±0.05)E-2										
1.371	(0.42 ±0.13)E-3										

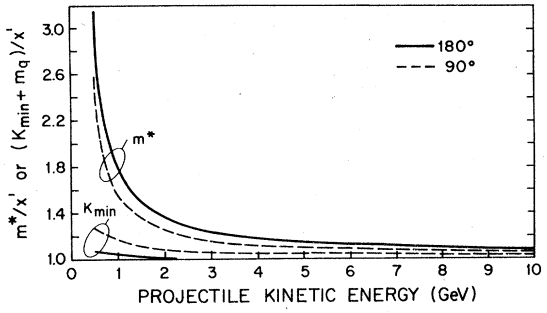

FIG. 1. The ratio of the cluster variable m^* and the QTBS variable $(k_{\min}+m_q)$, relative to the light cone variable $x'=(-q\cos\theta+E_q)M_a$, is shown vs the bombarding energy. All variables are identical when the incident energy reaches 400 GeV.

$+X$ at a laboratory angle of 160° vs the kinetic energy of the observed composite particle T_q. For values of T_q small enough so that an exponential form $\exp(-T_q/T_0)$ is a good approximation, one can parametrize the data obtained at any angle. Figure 3(a) shows values of T_0 for deuterons, tritons, and ^{3}He vs laboratory angle, along with values of T_0 for proton production obtained in the companion experiment of Ref. 10. In Fig. 3(b) the ratios $T_0(d)/T_0(p)$, $T_0(t)/T_0(p)$, and $T_0(^3\mathrm{He})/T_0(p)$ are also shown to allow evaluation of the variation of T_0 with particle type at all measured angles. For comparison with Fig. 2 we show in Fig. 4 a plot of $Ed^3\sigma/dq^3$ vs $k_{\min}$. The lines shown are from a fit to $\exp(-k_{\min}/k_0)$. For angles down to 90° laboratory, $k_{\min}$ is always positive, and we can display the results of our fits to this exponential

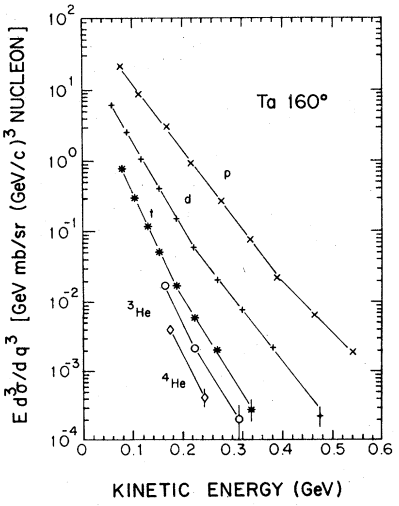

FIG. 2. Invariant cross sections per nucleon vs kinetic energy for d, t, ^{3}He, and ^{4}He: ^{181}Ta target at 160° laboratory angle.

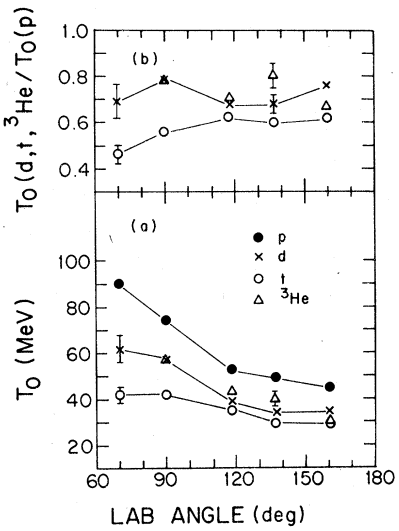

FIG. 3. (a) Values of T_0 from fits to $\exp(-T/T_0)$ for p, d, t, and ^{3}He at the various angles, Ta target. (b) Ratios of T_0 for d, t, and ^{3}He relative to T_0 for protons.

form vs angle.[14] Figure 5(a) shows values of k_0 for deuterons, tritons, and ^{3}He vs laboratory angle along with values of k_0 from proton production. In Fig. 5(b) the ratios $k_0(d)/k_0(p)$, $k_0(t)/k_0(p)$, $k_0(^3\mathrm{He})/k_0(p)$ are presented for comparison with Fig. 3(b).

Figure 6(a) shows typical plots of $Ed^3\sigma/dq^3$ per nucleon vs T_q for different angles for deuterons,

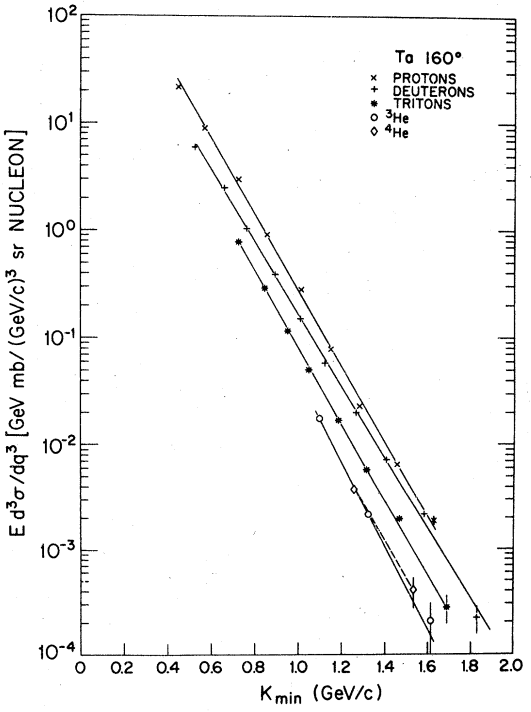

FIG. 4. $Ed^3\sigma/dq^3$ per nucleon vs $k_{\min}$ for that data in Fig. 2.

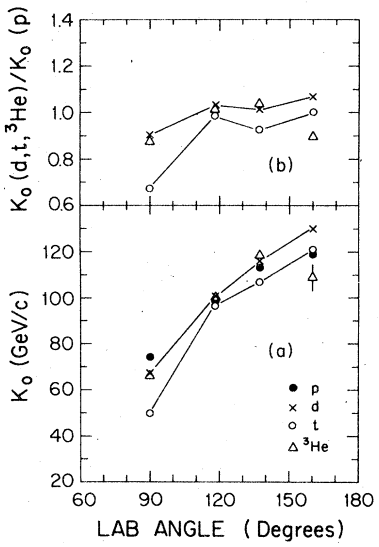

FIG. 5. (a) Values of k_0 from fits to $\exp(-k/k_0)$ for p, d, t, and ^{3}He at the various angles, Ta target. (b) Ratios of k_0 for d, t, and ^{3}He relative to k_0 for protons.

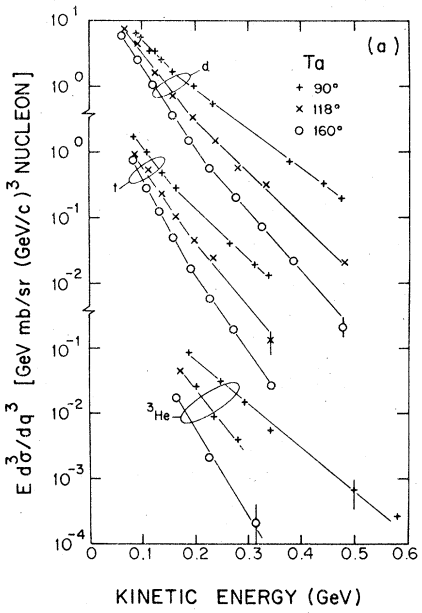

tritons, and ^{3}He, respectively, for Ta. Figure 6(b) shows plots of the same data vs $k_{\min} = -q\cos\theta + T_q$. Figures 7(c) and 7(b) show the A dependence of the invariant cross section *per nucleon* for deuterons and tritons, respectively, at 160°. Figure 7(a) shows the A dependence at 90° where we have the most data on ^{3}He production.

We now turn to an examination of the A dependence of our data derived from data at all angles, similar to those displayed in Fig. 7. It is not, in principle, possible to parametrize the magnitudes of the cross sections independently of specifying the energy of the observed particles since the shapes are not exactly A independent. Nevertheless, since the shapes are quite similar, and since the A dependence of the cross sections is an important guide to the construction of viable theories, we can study the A dependence, for example, at fixed T_q. In Fig. 8 we compare the A dependence of the cross sections for different particles and different angles. Because our data for Li is often of poorer quality than for C, where the statistical accuracies are better and background subtractions less important, we have chosen to present the ratios of all cross sections to the cross section for carbon. Since absolute values are not important here, we have further chosen to multiply these ratios by constants chosen to make the Li/C ratio approximately equal to unity so that the ratios for protons, deuterons, and tritons shown on our plots appear near $R = 1$. Thus, for example, we show the plot of $\log 2.8[d\sigma(A)/d\sigma(\text{carbon})]$ vs $\log A$ for protons while for deuterons and tritons the ratios have been multipled by the factors 3.5 and 5.0 respectively.

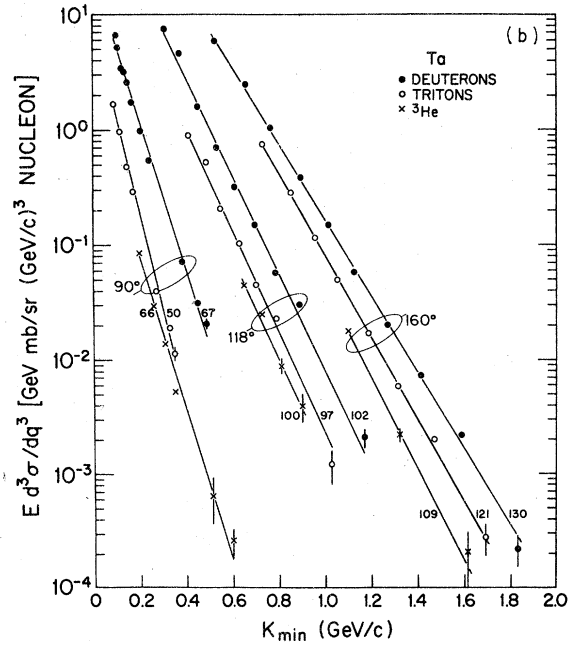

FIG. 6. (a) Invariant cross sections per nucleon vs kinetic energy for d, t, and ^{3}He at laboratory angles of 90°, 118°, and 160° for a Ta target. (b) The data of 6(a) is plotted vs $k_{\min}$ rather than T_q. The numbers next to the straight lines are the slopes (k_0) in units of MeV/c.

The choice of the value of T_q at which to compute the ratios $d\sigma(A)/d\sigma(\text{carbon})$ was motivated by our desire not to use extrapolations but to chose values of T_q where only smooth interpolations for all the A's could be employed. The values of T_q used for these plots are: protons—232 MeV; deuterons—

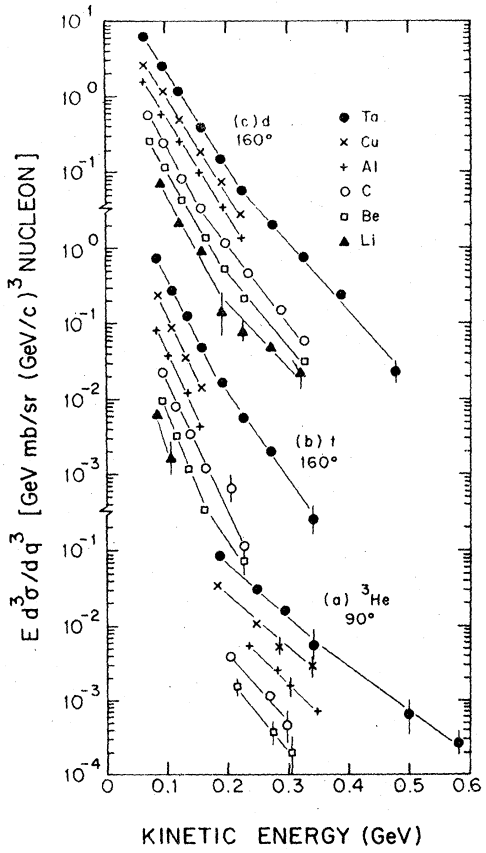

FIG. 7. Invariant cross section per nucleon vs kinetic energy for the various targets (a) ^{3}He at 90°, (b) t at 160°, (c) d at 160°.

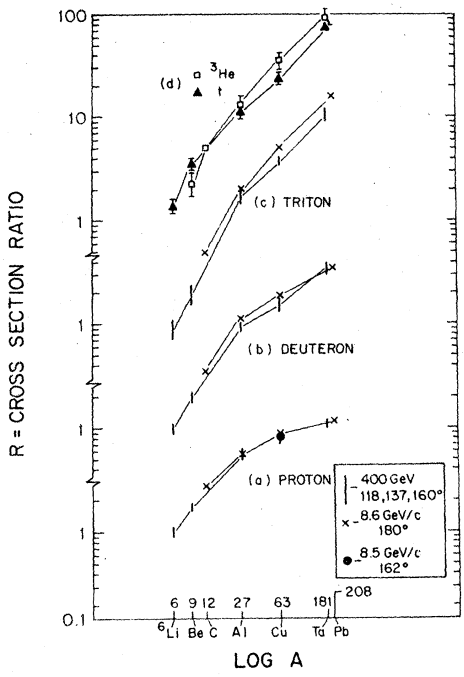

FIG. 8. The ratio (R) of the invariant cross section per nucleon for the various targets relative to that of carbon. Refer to text for the normalization used. The vertical lines in (a), (b), and (c) represent the spread in R over 118°, 137°, and 160°. 8.6 GeV/c (Ref. 15) and 8.5 GeV/c (Ref. 16) data are also displayed. (a) protons, T_q=232 MeV, (b) deuterons, T_q=100 MeV, (c) tritons, T_q=90 MeV, (d) 90° data for ^{3}He, T_q=250 MeV and tritons, T_q=125 MeV.

100 MeV; tritons—90 MeV. Our comparison of the A dependence of tritons with ^{3}He at 90° was made at the following values: tritons—125 MeV and ^{3}He—250 MeV. The vertical lines in 8(a)–(c) represent the spread in R over the 118°, 137°, and 160° angles, showing the insensitivity of the A dependence over these laboratory angles. This spread is comparable to the accuracy of the data. The 180°, 8.6 GeV/c, p, d, and t data[15] and 162° 8.5 GeV/c proton data[16] are also plotted. Figure 8(d) shows R for the 90° triton data and the 90° ^{3}He data, where the vertical bars represent the experimental errors.

Figure 9 shows the invariant cross section per nucleon vs T_q under various conditions of angle and incident energy for p, d, and t. The numbers positioned near the straight line are the straight line fits to the slope in MeV.

CONCLUSIONS

There are at present no published theoretical calculations for this high energy region on any model. Thus in this paper we restrict ourselves

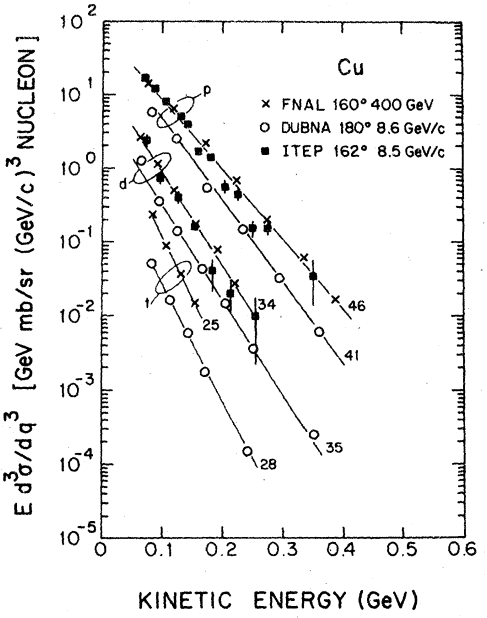

FIG. 9. Comparison of the invariant cross section per nucleon for this experiment, and that at 8.6 GeV/c (Ref. 15) and 8.5 GeV/c (Ref. 16) for a Cu target.

to data presentation and to some comparisons using different scaling variables. Below we summarize some of the main features:

(1) There is a strong *angular dependence* in the shape of the cross sections, when plotted vs T_q, for deuterons, tritons, and ^{3}He production, [see Fig. 6(a)] as is also observed for proton production.

(2) There is only a small, but nonvanishing, dependence *on* A, of the shapes of the cross section per nucleon for d, t, and ^{3}He production [see Figs. 7(a)–(c)], as is also observed for proton production.

(3) The ^{3}He and t cross sections have the same shapes, the relative cross sections reflecting the N/Z ratio in the Ta target. (See Fig. 2.)

(4) There is a large A dependence of the magnitude of the cross sections per nucleon on atomic mass number. This relative A dependence does not vary appreciably with backward angle and is the same at 8.5 GeV/c as at 400 GeV. (See Fig. 8.)

(5) The A dependence is strongest for the heaviest emitted fragments. For example per nucleon Ta produces 4 times as many protons, 10 times as many deuterons, and 20 times as many tritons as carbon. Tritons and ^{3}He with the same number of nucleons have a similar A dependence, i.e., for $d\sigma(A)/d\sigma(\mathrm{C})$.

(6) Almost all the data show departure of the invariant cross sections from the exponential form $\exp(-T_q/T_0)$. (See Fig. 2.)

(7) Parametrization of the cross sections per nucleon in terms of T_0 shows different values of T_0 for protons, deuterons, and tritons. [See Fig. 3(b).] Parametrization in terms of $k_{\min}$ shows less change for different ions [see Fig. 5(b)], the ratios for the most backward angles hovering about unity. This latter behavior shows up at the low incident energies of 0.6 and 0.8 GeV, as well.[2]

(8) Figure 6(b) shows that the shapes of the cross sections vs $k_{\min}$ are similar for d, t, and ^{3}He but have a residual angular dependence. This is to be qualitatively expected from the "single scattering hypothesis,"[1-3] the smaller magnitude, and faster falloff at 90° relative to 160°, reflecting the larger momentum transfers at 90° ($t \sim q_\perp^2$ at 400 GeV.)

(9) Figure 9 shows that the shapes and magnitude of the cross sections per nucleon for both protons and deuterons at almost the same angles, 160° at 400 GeV and 162° at 8.5 GeV/c, are identical. We have also plotted the 180° data at 8.6 GeV/c for the deuterons and tritons showing similar shapes but a drop of about a factor of 3 in the cross sections at the more backward angle. The same drop is found in the comparison of the triton data shown in Fig. 9; no 8.5 GeV/c 162° triton data is available. Thus from Fig. 9 we may conclude that the shapes and magnitudes of the cross sections for production of light ions (d, t) as well as protons appear to be energy independent over this 50:1 energy variation of the incident proton.

ACKNOWLEDGMENTS

We wish to thank D. Ritchie and L. Taff for their help in assisting us to incorporate the Fermilab MULTI into the on-line analysis of our experiment. In particular we thank the members of the Fermilab Proton Department for their enthusiastic cooperation. This work was supported in part by the Department of Energy and the National Science Foundation, U.S.A., and the State Committee on the Utilization of Atomic Energy, U.S.S.R.

[1] R. D. Amado and R. M. Woloshyn, Phys. Rev. Lett. 36, 1435 (1976).
[2] S. Frankel, Phys. Rev. Lett. 38, 1338 (1977).
[3] I. A. Schmidt and R. Blankenbecler, Phys. Rev. D 15, 3321 (1977).
[4] L. L. Frankfurt and M. I. Strikman, Phys. Lett. 83B, 407 (1979).
[5] A. M. Baldin, Fiz. Elem. Chastits At. Yadra 8, 429 (1979) [Sov. J. Part. Nucl. 8, 175 (1977)].
[6] T. Fujita, Phys. Rev. Lett. 39, 174 (1977).
[7] R. M. Woloshyn, Nucl. Phys. A306, 333 (1978).
[8] V. V. Burov, V. K. Lukyanov, and A. I. Tito, Phys. Lett. 67B, 46 (1977).
[9] T. Fujita and J. Hüfner, Nucl. Phys. A314, 317 (1979).
[10] Y. D. Bayukov *et al.*, Phys. Rev. C 20, 764 (1979).
[11] G. P. Millburn *et al.*, Phys. Rev. 95, 1268 (1954).
[12] G. A. Leksin, ITEP 147, International Conference on High Energy Physics, 1976 (unpublished).
[13] S. Frankel, Phys. Rev. C 17, 694 (1978).
[14] At angles forward of 90° the factorization of cross sections into constituent-constituent interactions and structure functions (see Refs. 2, 3, and 10) is not likely to be valid. In fact, because of the high multiplicity in $p+p$ collisions at 400 GeV and the very strong A dependence of the cross sections, it is not certain that the 90° data does not contain contributions from more forward single scattering angles.
[15] A. M. Baldin *et al.*, JINR PI-11302, Dubna (unpublished).
[16] N. A. Burgov *et al.*, ITEP-147 (unpublished).